

ADA 132060

12

OFFICE OF NAVAL RESEARCH

Contract N00014-76-C-0408

Project NR 092-555

Technical Report No. 29

FAILURE PROCESSES IN ELASTOMERS AT OR
NEAR A RIGID SPHERICAL INCLUSION

by

A. N. Gent and Byoungkyeu Park

Institute of Polymer Science
The University of Akron
Akron, Ohio 44325

September, 1983

SEP 2 1983

Reproduction in whole or in part is permitted
for any purpose of the United States Government

Approved for Public Release; Distribution Unrestricted

DTIC FILE COPY

83 09 02 003

REPORT DOCUMENTATION PAGE		READ INSTRUCTIONS BEFORE COMPLETING FORM
1. REPORT NUMBER Technical Report No. 29	2. GOVT ACCESSION NO. AD-A132 060	3. RECIPIENT'S CATALOG NUMBER
4. TITLE (and Subtitle) Failure Processes In Elastomers At Or Near A Rigid Spherical Inclusion		5. TYPE OF REPORT & PERIOD COVERED Technical Report
		6. PERFORMING ORG. REPORT NUMBER
7. AUTHOR(s) A. N. Gent and Byoungkyeu Park		8. CONTRACT OR GRANT NUMBER(s) N00014-76-C-0408
9. PERFORMING ORGANIZATION NAME AND ADDRESS Institute of Polymer Science The University of Akron Akron, Ohio 44325		10. PROGRAM ELEMENT, PROJECT, TASK AREA & WORK UNIT NUMBERS NR 092-555
11. CONTROLLING OFFICE NAME AND ADDRESS Office of Naval Research Power Program Arlington, VA 22217		12. REPORT DATE September, 1983
		13. NUMBER OF PAGES
14. MONITORING AGENCY NAME & ADDRESS (if different from Controlling Office)		15. SECURITY CLASS. (of this report) Unclassified
		15a. DECLASSIFICATION/DOWNGRADING SCHEDULE
16. DISTRIBUTION STATEMENT (of this Report) According to attached distribution list. Approved for public release; distribution unrestricted.		
17. DISTRIBUTION STATEMENT (of the abstract entered in Block 20, if different from Report)		
18. SUPPLEMENTARY NOTES Submitted for publication in: Journal of Materials Science		
19. KEY WORDS (Continue on reverse side if necessary and identify by block number) Adhesion, Cavitation, Debonding, Detachment, Elastomers, Failure, Fracture, Glass beads, Inclusion, Rubber, Rupture, Tensile stress, Vacuoles.		
20. ABSTRACT (Continue on reverse side if necessary and identify by block number) — A systematic experimental study has been carried out of two distinct failure phenomena, cavitation and debonding, in an elastomer containing a rigid spherical inclusion. Several elastomers were employed containing glass beads of various diameters, ranging from 60 μm to 5000 μm , and with chemically- different surfaces. The critical stress for cavitation was found to depend upon Young's modulus E of the elastomer and upon the diameter of the bead. By extrapolation, it was found that the stress for cavitation near an -- >		

20.

infinitely-large bead is given by $5E/12$, as predicted by theory. In contrast the critical stress for debonding decreased somewhat with increasing Young's modulus of the elastomer. This is attributed to a concomitant decrease in the strength of adhesion between the elastomer and the bead surface, due to rheological effects. The stresses for both cavitation and for debonding were found to vary approximately with the negative half-power of the bead diameter. This suggests that a similar Griffith mechanism governs both failure processes when the bead size is small.

A study of cavitation and debonding in the presence of two glass beads was also carried out. As predicted from theoretical considerations, both stresses were found to decrease as the distance between the two beads was decreased, irrespective of the diameter of the bead and Young's modulus of the elastomer. At higher strains, however, a second cavitation process was found to take place at a point midway between the beads. Tensile fracture of the specimen resulted from the unrestrained lateral growth of the second cavity.

Failure Processes In Elastomers At Or Near

A Rigid Spherical Inclusion

A. N. Gent and Byoungkyeu Park

Institute of Polymer Science

The University of Akron

Akron, Ohio 44325

Abstract

A systematic experimental study has been carried out of two distinct failure phenomena, cavitation and debonding, in an elastomer containing a rigid spherical inclusion. Several elastomers were employed containing glass beads of various diameters, ranging from $60 \mu\text{m}$ to $5000 \mu\text{m}$, and with chemically-different surfaces. The critical stress for cavitation was found to depend upon Young's modulus E of the elastomer and upon the diameter of the bead. By extrapolation, it was found that the stress for cavitation near an infinitely-large bead is given by $5E/12$, as predicted by theory. In contrast, the critical stress for debonding decreased somewhat with increasing Young's modulus of the elastomer. This is attributed to a concomitant decrease in the strength of adhesion between the elastomer and the bead surface, due to rheological effects. The stresses for both cavitation and for debonding were found to vary approximately with the negative half-power of the bead

diameter. This suggests that a similar Griffith mechanism governs both failure processes when the bead size is small.

A study of cavitation and debonding in the presence of two glass beads was also carried out. As predicted from theoretical considerations, both stresses were found to decrease as the distance between the two beads was decreased, irrespective of the diameter of the bead and Young's modulus of the elastomer. At higher strains, however, a second cavitation process was found to take place at a point midway between the beads. Tensile fracture of the specimen resulted from the unrestrained lateral growth of the second cavity.



Accession For	
NTIS GRA&I	<input checked="" type="checkbox"/>
DACS TM	<input type="checkbox"/>
Unannounced	<input type="checkbox"/>
Justification	
Description/	
Availability Codes	
Avail and/or	
Special	

Introduction

Elastomers are commonly reinforced by the incorporation of relatively large amounts, 30-50 per cent by volume, of finely-divided rigid fillers such as carbon black. The exact mechanism of reinforcement is still obscure, however. In an attempt to clarify it, a detailed study has now been carried out of the micromechanics of tensile failure in a sample containing a single rigid spherical inclusion. Some observations have also been made with two spherical inclusions placed close together in the direction of the applied tension, in order to study the effect of particle propinquity upon the mode of failure.

Two modes of failure have been noted previously in filled elastomers. When transparent elastomers containing fillers are stretched, vacuoles are commonly found to appear at a critical extension (1-3). This phenomenon has been generally referred to as "dewetting" and attributed to detachment of weakly-bonded elastomer from the surface of filler particles. On the other hand, Oberth and Bruenner (4) showed that a small vacuole is formed near, but not at, the surface of a large rigid spherical inclusion when the elastomer was bonded to the inclusion sufficiently well to resist detachment. Elastomers undergo a characteristic failure process, termed cavitation, when subjected to a sufficiently large triaxial tension (negative hydrostatic

pressure), given approximately by $\frac{5E}{6}$ where E is Young's modulus (5). This process consists of the unbounded elastic expansion of a microvoid, assumed to be present initially in all elastomers, until material at its surface reaches the breaking elongation. The cavity then grows in a catastrophic way until it is large enough to relieve the triaxial tension by its presence.

A triaxial tension is developed near the poles of a spherical inclusion, of magnitude $2t_{\infty}$ where t_{∞} is the tensile stress applied at infinity (6), Figure 1. We therefore expect vacuoles to appear near the poles of the inclusion when the applied stress reaches a value of $\frac{5E}{12}$. Oberth and Bruenner observed a direct proportionality between the stress for vacuole formation and Young's modulus of approximately this form, i.e., $\frac{E}{2}$, by experiments with polyurethane elastomers having a wide range of values of Young's modulus E , containing a single spherical inclusion with a diameter of about 6 mm. They also found that dewetting took place subsequently, if at all, by growth of cavities towards the surface of the inclusion.

Thus, for well-bonded systems the initial failure appears to take place near the inclusion by internal rupture of the elastomer under the action of a triaxial tension, whereas for weakly-bonded systems it appears to take place by detachment of the elastomer from the surface of the inclusion. Examples

of these failure processes are shown in Figure 2. The precise criteria for either process to occur are not really well-understood, however. At what level of bonding is one process superceded by the other? Does the failure stress for either process depend upon the size of the inclusion? And how are these processes altered when inclusions are placed in close proximity? Experiments designed to address these questions have now been carried out, using transparent elastomers containing small glass beads. The diameter of the beads was varied over a wide range, 60-5000 μm . The strength of adhesion between a bead and the elastomeric matrix was also adjusted by treating the bead either with a coupling agent or with a release agent before use. Several different elastomers were employed. In each case the elastic modulus was varied by varying the degree of molecular interlinking; values of Young's modulus E were obtained in this way ranging from 0.9 to 3.0 MPa. Observations of various failure processes and experimentally-determined values of the corresponding failure stresses are reported below.

Experimental Details

Elastomers

Several different elastomers were used in the experiments: two types of polybutadiene (Cis-4 1203, Phillips Petroleum Company, and Diene 35 NFA, Firestone Rubber and Latex Company), two types of cis-polyisoprene (SMR-5L, Malaysian natural rubber, and Natsyn 2200, Goodyear Tire and Rubber Company) and a castable silicone rubber compound (Sylgard S-184, Dow Corning Corporation). The first four materials were crosslinked by adding various amounts of dicumyl peroxide and then heating the mixture in a mold to produce crosslinked rubber slabs containing one or two centrally-located glass beads, inserted before crosslinking. The silicone rubber was crosslinked using a reagent (Sylgard C-184) supplied by Dow Corning Corporation, which was added to the elastomer in various proportions. The mixture was then poured into a glass tray and crosslinked by heating for 24 h at 110°C. Glass beads were placed in the center of the sheet after 15 min, i.e., before much crosslinking had taken place.

All of these materials had in common a high degree of transparency, so that cavitation near, or detachment from, the inclusion could be observed directly (Figure 2).

Rigid spherical inclusions

Soda-lime glass beads were used as rigid inclusions. They were washed with boiling isopropyl alcohol, dried, and inserted

in the center of the rubber strips before crosslinking them. In order to obtain strong adhesion to diene elastomers, some beads were treated with a dilute solution of vinyltriethoxysilane in water, using acetic acid as a catalyst for hydrolysis of the ethoxy groups. They were then heated for 30 min at 110°C. To obtain poor adhesion to diene elastomers, ethyltriethoxysilane was used instead of the vinyl silane. The vinyl group appears to form a covalent bond with the elastomer during crosslinking with dicumyl peroxide, but the ethyl group does not (7).

In order to obtain strong and weak adhesion to the silicone elastomer, glass beads were treated with a special primer (92-023, Dow Corning Corporation) and a dilute solution of non-ionic surfactant (Triton X-105) in ethanol, respectively.

Measurement of failure stresses

Measurements were made of the applied tensile stress t_c at which the first visible cavity appeared, and of the stress t_a at which sudden debonding occurred, if debonding took place before any cavity formed. These stresses were applied to the ends of a long parallel-sided strip of the elastomer, having the inclusion at its center. The thickness and width of the strip were at least three times the diameter of the inclusion, and usually much larger, so that the inclusion was effectively contained within an infinitely-large block, subjected to simple extension. Quite large extensions, of the

order of 50-400 per cent, were imposed before failure. They were especially large for cavitation near a small-diameter inclusion, well-bonded to a soft elastomeric material. Now, rubbery materials generally follow non-linear relations between tensile stress and extension, as shown in Figure 3 for some of the materials used in the present experiments. Values of Young's modulus E can be obtained from the initial slopes of such relations, but the stresses near an inclusion calculated from linear elasticity theory are unlikely to be accurate for non-linear materials when the imposed strains are large. It should be noted that Oberth and Bruenner used engineering stress (applied force per unit of unstrained cross-sectional area) in comparing their measured cavitation stresses with theoretical predictions (4). As their materials were stretched significantly under these stresses, by 50-100 per cent, the true applied stresses were considerably larger than the values they quote, by the same proportion.

In Figure 4, the relations between true tensile stress t and extension e are shown for some of the elastomers used. These relations are substantially linear in many cases, even up to strains of 200-300 per cent. Thus, the conclusions of linear elasticity theory might well apply, at least to a first approximation, to the high stresses set up near a rigid inclusion in a highly-stretched elastomer.

Experimental Results and Discussion

Failure processes with a single inclusion

With well-bonded inclusions a small cavity formed near one pole of the inclusion in the direction of the applied tension, Figure 2a, when the applied stress reached a critical level. On further elongation the cavity grew in size to touch the glass bead and several other cavities appeared at both poles, Figure 5. They grew somewhat in the tension direction as the strain was increased further until the test piece broke in two, usually initiated from a cavity.

With less-well-bonded inclusions an abrupt debonding took place after the cavities had already appeared, as shown in Figure 6. In these cases, a lateral crack was sometimes observed to form subsequently in the elastomer near the edges of the debonded region. It grew slowly until it escaped from the immediate vicinity of the inclusion, when catastrophic failure ensued.

With unbonded inclusions the initial failure event was a sudden detachment at one side of the inclusion, Figure 2b, followed at much larger strains by the appearance of a smaller debonded void at the other side of the inclusion, Figure 7. Fracture again resulted from the growth of a lateral crack, initiated near the edge of the debonded region.

Cavitation stresses

The critical value of the applied force f_c per unit undeformed cross-sectional area at which the first cavity was observed, is plotted in Figure 8 against Young's modulus E , for five different materials. At first sight, these results appear to be in reasonable agreement with the theoretical predictions of Oberth and Bruenner, represented by the broken line in Figure 8. However, the use of nominal applied stress in place of true tensile stress does not seem appropriate. There are substantial quantitative differences between these two measures of stress for highly-deformed materials, so that the apparent agreement shown in Figure 8 is lost when true stresses are employed, Figure 9. Furthermore, the stresses at which cavitation occurs near small inclusions are much greater than for large ones, as discussed below, so that the apparent numerical agreement shown in Figure 8 fails to hold for inclusions of other sizes.

When the true stresses t_c for cavitation are plotted against the corresponding values of Young's modulus E , linear relations are obtained with slopes approximately equal to the theoretical value $5/12$ but displaced to higher stresses as the diameter of the inclusion is reduced, Figures 9 and 10. Moreover, the stresses for cavitation in Natsyn 2200 appear to be significantly higher than for all of the other materials under similar conditions. This feature is discussed later.

It was found that all of the cavitation stresses could be represented quite well by a relation of the Hall-Petch form (8,9):

$$t_c = AE + Bd^{-1/2} \quad (1)$$

where A and B are constants and d denotes the diameter of the glass bead. Some representative results are plotted in this way in Figure 11; satisfactorily linear relations were obtained, with slopes B of 40 kPa.m^{1/2} for Natsyn 2200 and 25 kPa.m^{1/2} for all of the other elastomers, and an intercept corresponding to a value of A of about 0.5.

The term AE in equation 1 is attributed to the elastic resistance to infinite expansion of a small spherical void in an elastomer subjected to triaxial tension (5). It is hypothesized that such microscopically-small voids exist in all elastomers. Moreover, it is known that the stress field near the poles of a rigid spherical inclusion is a triaxial tension, of magnitude $2t_\infty$ where t_∞ is the tensile stress applied at infinity; see Figure 1. Thus, a failure criterion for cavitation of the form

$$t_c = 5E/12 \quad (2)$$

is expected to be generally applicable (4). However, it now appears that this criterion is only valid for relatively-large inclusions. It becomes increasingly inadequate as the size of the inclusion is reduced and the second term on the right-hand side of equation 1 becomes increasingly important.

This second term resembles the Griffith criterion (10) for growth by tearing of a small circular crack of diameter \underline{c} in the material close to the inclusion, where the tensile stress is $2t$ (6),

$$2t_c = (2\pi E G_c / 3\sigma)^{1/2} \quad (3)$$

In this relation G_c denotes the energy required to propagate a crack by tearing through unit area of material. Values of the tearing energy G_c were measured for the various elastomers. They were found to range from about 500 to about 5000 J/m².

Thus, it appears that the formation of a visible cavity near a small inclusion of diameter \underline{d} involves the growth by tearing of a small defect of diameter \underline{c} , where \underline{c} is found to be proportional to \underline{d} . Putting $\underline{c} = \underline{\alpha d}$ to denote this proportionality, the magnitude of the constant $\underline{\alpha}$ can be estimated by comparing the experimental values of the slopes \underline{B} in equation 1 with the predictions of equation 3. When this is done, using a representative value for \underline{E} of 1.5 MPa, the value obtained for $\underline{\alpha}$ is found to be improbably large, of order unity. Defects comparable in size to the inclusion itself would certainly not escape notice in the experiments. It is therefore concluded that equation 3 does not hold for the propagation of a small crack near a rigid inclusion in an elastomer under tension.

Several reasons for this failure can be postulated. The elastomer near the inclusion is not under a simple tensile

stress, and equation 3 may be invalid in this case. The initial defects are inherently small and values of G_c obtained by tearing apart large specimens may not apply to microscopic tearing processes. Also, it is known that stretched elastomers tear much more easily in the stretching direction so that much lower values of G_c will apply to tears running in the direction of the applied tension (11). Whatever the reason, it is clear that there is a strong dependence of the critical stress for cavitation upon the size of the rigid inclusion and that the critical stresses, although quite large for small inclusions, are unexpectedly low when a Griffith tearing criterion is applied (equation 3).

The cavitation stresses are significantly higher for Natsyn 2200 than for the other elastomers examined and this observation may provide a useful clue on the origin of the size-dependence. Although Natsyn 2200 is closely similar to natural rubber (SMR-5L), it does not crystallize as readily on stretching. Consequently, it probably shows a different level of anisotropy of tear strength in the stretched state. A further experimental study of this feature would be illuminating.

Debonding stresses

Observations were also made of the critical applied stress t_a at which the elastomer pulled away from a weakly-bonded inclusion. For an inclusion of a given size, the debonding stress was found to be smaller for harder elastomers, in marked contrast to the increase of cavitation stress t_c with elastomer modulus discussed in the preceding section. The two failure processes are thus quite distinct, Figure 12.

It is at first sight surprising that the debonding stress should decrease with Young's modulus E of the elastomer, as shown in Figure 12, because a simple Griffith treatment of the mechanics of debonding yields the relation (12)

$$t_a = (8\pi E G_a / 3d \sin 2\theta)^{1/2} \quad (4)$$

where G_a denotes the energy required to detach the elastomer per unit area of interface and 2θ denotes the angle subtended by a hypothetical initially-debonded circular patch on the inclusion, located at the pole, i.e., in the direction of the applied tension. Equation 4 suggests that the debonding stress will increase with an increase in E . However, it is commonly found that the work G_a of detachment of an elastomer from a rigid surface is greatly dependent upon the dissipative properties of the elastomer, being greater for more dissipative materials (13). Now, harder elastomers, obtained by incorporating a greater density of intermolecular

bonds, are less dissipative than softer materials and show a lower strength of adhesion (13,14). This was found to be the case also for the present materials. Thus, the term G_a in equation 4 is reduced drastically as the term E is increased and the net effect is a reduction in debonding stress as the elastomer is made harder.

Since the detachment energy G_a is also strongly dependent upon the rate of detachment, it is rather difficult to make a quantitative comparison with the predictions of equation 4. If it is assumed that the rate of propagation of the initial debond is about 10^{-5} m/s, then the measured value for G_a of about 17 J/m^2 for a silicone elastomer S-184 peeled from a detergent-treated glass plate at this rate leads to a value for the subtended angle θ of about 7.5° , using the measured debonding stress for a $200 \mu\text{m}$ bead of about 2 MPa, and Young's modulus for this elastomer of about 2.2 MPa, in equation 4.

This value of θ is a measure of the area of the hypothetical initially-debonded patch upon the surface of the inclusion which grows in a catastrophic way when the applied tensile stress reaches the critical value t_a . When inclusions of different size were used, the debond stress t_a was found to vary markedly, being much larger for smaller inclusions, as discussed next. Surprisingly, these results are consistent with a substantially-constant value for θ ,

independent of the size of the inclusion. This suggests that θ does not, in fact, represent a specific defect at the interface between the elastomer and the inclusion, because it seems highly unlikely that the area of a debonded patch would prove to be proportional to the surface area of the inclusion itself, over wide ranges of size. Instead, it seems likely that θ represents a characteristic feature of the mechanics of debonding from spherical inclusions.

Measured values of debonding stress t_a are plotted in Figure 13 against the diameter of the glass bead raised to the negative half-power, in accordance with equation 4. Results for three different elastomers are shown. In all cases, the debonding stress was found to increase as the size of the inclusion was decreased, approximately in accordance with a negative half-power. Thus, as for cavitation stresses, debonding stresses also appear to follow a Griffith-type relation in terms of the size of the inclusion. However, the slopes of the relations shown in Figure 13 are somewhat smaller than those for cavitation (Figure 11) and the relations appear to pass through the origin, rather than extrapolating to yield a finite value of t_a for infinitely-large inclusions.

Failure processes with two inclusions

The progress of cavitation in the vicinity of two inclusions having their centers arranged along the tension axis took a characteristic and distinctive form. First, at a critical stress somewhat lower than that necessary to cause a void to appear near an isolated inclusion, small cavities formed near the inner poles, Figure 14. Apparently, the triaxial stress developed at these points is somewhat greater than $2t$ when the inclusions are closely spaced.

Then, at a somewhat higher value of applied stress, a large cavity suddenly appeared midway between the two inclusions. A similar phenomenon takes place in thin elastomer cylinders bonded between rigid plates and placed under tension (5). It is attributed to the unbounded expansion of an initially-present microscopic void under the action of the triaxial tension present in the interior of the cylinder. Apparently, a similar stress field is developed between two rigid spherical inclusions and also leads to the formation of a large void.

The second cavity was found to be quite stable, growing slowly as the applied stress was increased, Figure 14, until it emerged from the gap between the two inclusions. At this point, it grew catastrophically, leading to rupture of the specimen.

A second example of cavity formation between two inclusions is shown in Figure 15. In this case the spacing of the inclusions was rather larger and the final cavity grew rapidly, causing rupture.

From these observations it seems clear that tensile rupture of specimens containing rigid inclusions is generally caused by the second cavitation process, occurring between inclusions, rather than the first, occurring near the poles of isolated inclusions. The latter cavities only grow in the direction of the applied tension, Figure 5, and thus do not lead directly to rupture.

Conclusions

The existence of two distinct failure phenomena, cavitation and debonding, has been clearly demonstrated using transparent elastomers containing glass beads of various sizes.

The critical stress for cavitation was found to depend on the Young's modulus of the elastomer and on the diameter of the glass bead. By extrapolation, the critical stress for cavitation near an infinitely-large bead is found to be linearly dependent on the Young's modulus of the elastomer, $t_c = 5E/12$, in accord with a simple theory of cavitation in which surface and fracture energies are neglected (5). The dependence of the cavitation stress on the diameter of the bead takes a Griffith form, being proportional to the negative half-power of the bead diameter. However, the measured stresses are lower than expected for precursor defects much smaller than the inclusion itself, as observation requires. This anomaly calls for further study.

The critical stress for debonding increases as the strength of adhesion between the elastomer and the bead was increased, as predicted by theory. On the other hand, it decreased with increasing Young's modulus of the elastomer. This anomaly is attributed to a decrease in the strength of adhesion between the elastomer and the bead as Young's modulus of the elastomer is increased. It was also found that the

critical stress for debonding was strongly dependent on the diameter of the bead, in accord with a Griffith-type relation:

$$t_a = (8\pi EG_a/3d \sin 2\theta)^{1/2}$$

This suggests that the effective initial debond angle θ is approximately independent of the diameter of the bead, $\theta = 10^\circ \pm 5^\circ$. This implies that θ does not represent a real defect at the surface of the inclusion, but a mechanical feature of debonding from a spherical surface.

For two beads in close proximity, a second cavitation process was observed midway between them, at a stress which decreased as the distance between the beads was decreased. This second cavity grew at right angles to the applied stress and led to catastrophic rupture of the specimen once it had escaped from the restraining influence of the inclusions. In contrast, cavities and debonds formed at the poles of isolated inclusions, grew in the direction of the applied tension, so that they did not lead directly to rupture.

References

1. H. F. Schippel, *Industr. Engng Chem.* 12, 33 (1920).
2. H. A. Depew and M. K. Easley, *Industr. Engng Chem.* 26, 1187 (1934).
3. C. Markins and H. L. Williams, *J. Appl. Polymer Sci.* 18, 21 (1974).
4. A. E. Oberth and R. S. Bruenner, *Trans. Soc. Rheol.* 9, 165 (1965).
5. A. N. Gent and P. B. Lindley, *Proc. Roy. Soc. (London)* A249, 195 (1959).
6. J. N. Goodier, *Trans. ASME* 55, 7 (1933).
7. A. Ahagon and A. N. Gent, *J. Polymer Sci. Polymer Phys. Ed.* 13, 1285 (1975).
8. E. O. Hall, *Proc. Phys. Soc. (London)* 64B, 747 (1951).
9. N. J. Petch, *J. Iron Steel Inst. London*, 174, 25 (1953).
10. R. A. Sack, *Proc. Phys. Soc. (London)* 58, 729 (1946).
11. A. N. Gent and H. J. Kim, *Rubber Chem. Technol.* 51, 35 (1978).
12. A. N. Gent, *J. Materials Sci.* 15, 2884 (1980).
13. A. N. Gent and R. P. Petrich, *Proc. Roy. Soc. (London)* A310, 433 (1969).
14. A. N. Gent and G. R. Hamed, *Plastics and Rubber: Materials and Applications* 3, 17 (1978); reprinted in *Rubber Chem. Technol.* 51, 354 (1978).

Figure Captions

- Figure 1. Stresses t_{RR} , $t_{\theta\theta}$, $t_{\phi\phi}$ near a rigid spherical inclusion as a function of distance from the surface of the inclusion in the direction of the applied tensile stress t_{∞} (6).
- Figure 2. Cavitation and debonding at the surface of a spherical inclusion in an elastic matrix under tension. Direction of applied tension: vertical. Diameter of inclusion: 1.2 mm.
- Figure 3. Representative relations between applied tensile force f per unit undeformed cross-sectional area and extension e . 1, S-184; 2, SMR-5L; 3, Cis-4.
- Figure 4. Representative relations between tensile stress t and extension e . 1, S-184; 2, SMR-5L; 3, Cis-4.
- Figure 5. Progress with increasing tensile strain of cavitation in a silicone elastomer (S-184) $E = 0.9$ MPa, containing a glass bead of 1.22 mm diameter bonded to the elastomer with a primer.
- Figure 6. Progress with increasing tensile strain of cavitation in a silicone elastomer (S-184) $E = 2.2$ MPa, containing an untreated glass bead of 610 μm diameter.
- Figure 7. Progress with increasing tensile strain of debonding in natural rubber (SMR-5L) $E = 1.6$ MPa, containing an ethylsilane-treated glass bead of 610 μm diameter.

Figure 8. Nominal tensile stress f_c (force per unit of undeformed cross-section) at which the first cavity was observed in five elastomers containing a glass bead of diameter 600 μm , plotted against Young's modulus E .

Natsyn-2200, \blacksquare ; S-184, Δ ; SMR-5L, \blacklozenge ; Cis-4, \bullet ; Diene 35 NFA, \blacktriangle .

Figure 9. Applied tensile stress t_c at which the first cavity was observed in five elastomers containing a glass bead of diameter 600 μm , plotted against Young's modulus E . The symbols have the same significance as in Figure 8.

Figure 10. Applied tensile stress t_c for void formation vs Young's modulus E for samples of Cis-4 containing glass beads of various diameters d .

The dotted line represents the theoretical relation, equation 2.

Figure 11. Applied tensile stress t_c for void formation vs $d^{-1/2}$, where d is the diameter of the glass bead inclusion. Natsyn 2200, \blacksquare ; Cis-4, \bullet .

Figure 12. Applied tensile stress for void formation t_c or detachment t_a vs Young's modulus E for samples of Natsyn 2200 containing a glass bead, diameter 600 μm .

Bonded, \blacksquare ; untreated, \square ; treated with ethylsilane, \blacktriangleleft .

Figure 13. Applied tensile stress t_a for debonding vs $d^{-1/2}$, where d is the diameter of the glass bead inclusion. S-184, Δ ; Diene 35NFA, \blacktriangle ; Cis-4, \bullet .

Figure 14. Progress of cavitation in a silicone elastomer, $E = 2.2$ MPa, containing two glass beads of 1.25 mm diameter bonded to the elastomer. Direction of applied tension: vertical.

Figure 15. Progress of cavitation in a silicone elastomer, $E = 3.0$ MPa, containing two glass beads of 1.25 mm diameter bonded to the elastomer. Direction of applied tension: vertical.

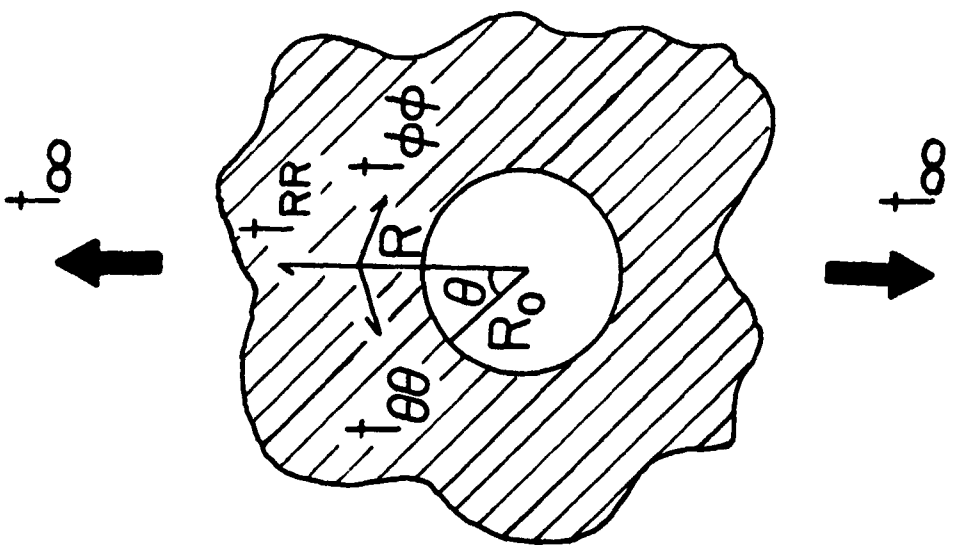
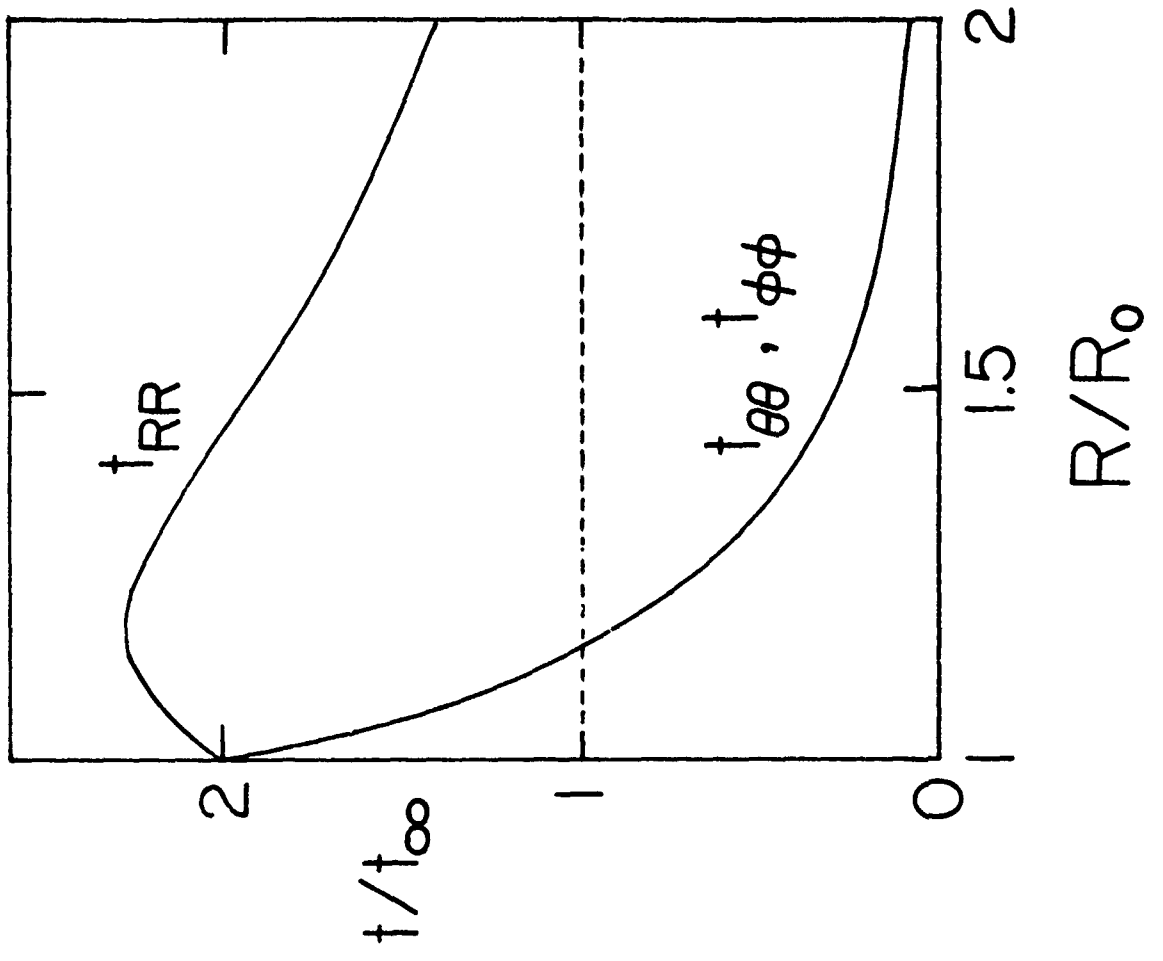
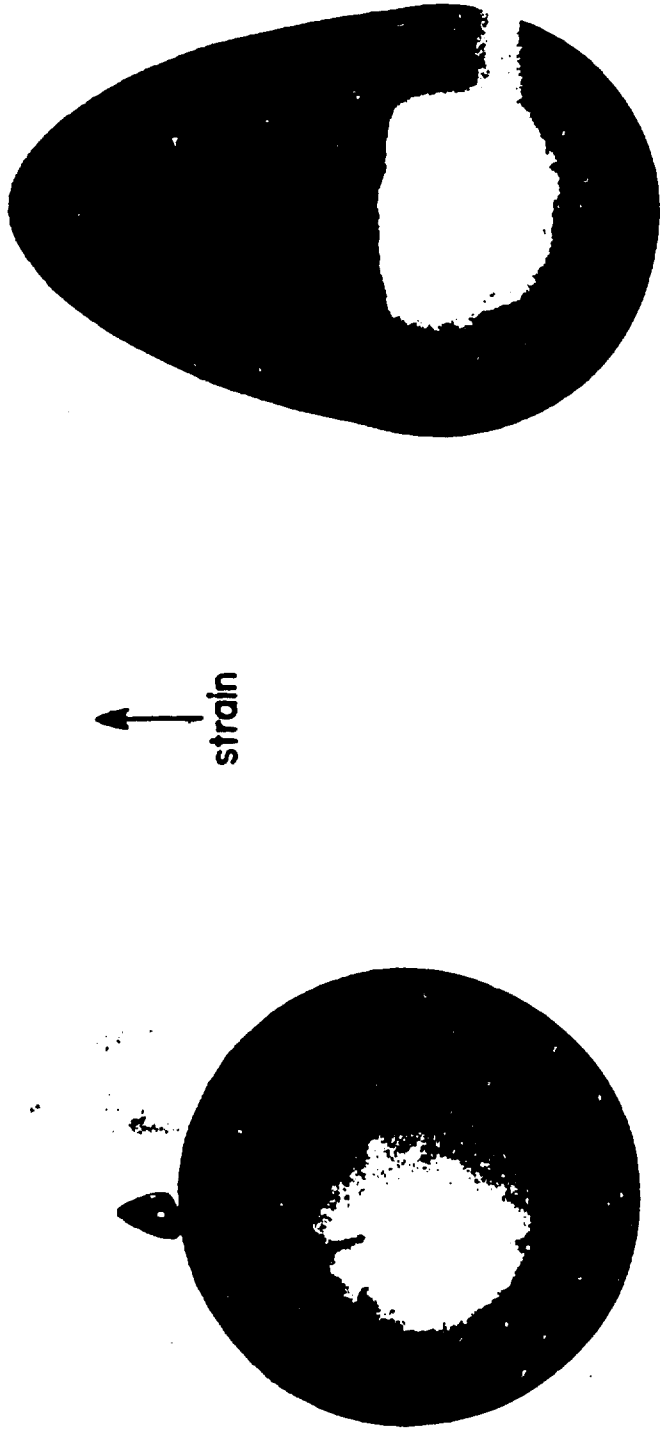


Figure 1.

CAVITATION

DEBONDING



a Glass Bead ($d=1200\mu\text{m}$) in Silicone Elastomer

Figure 2.

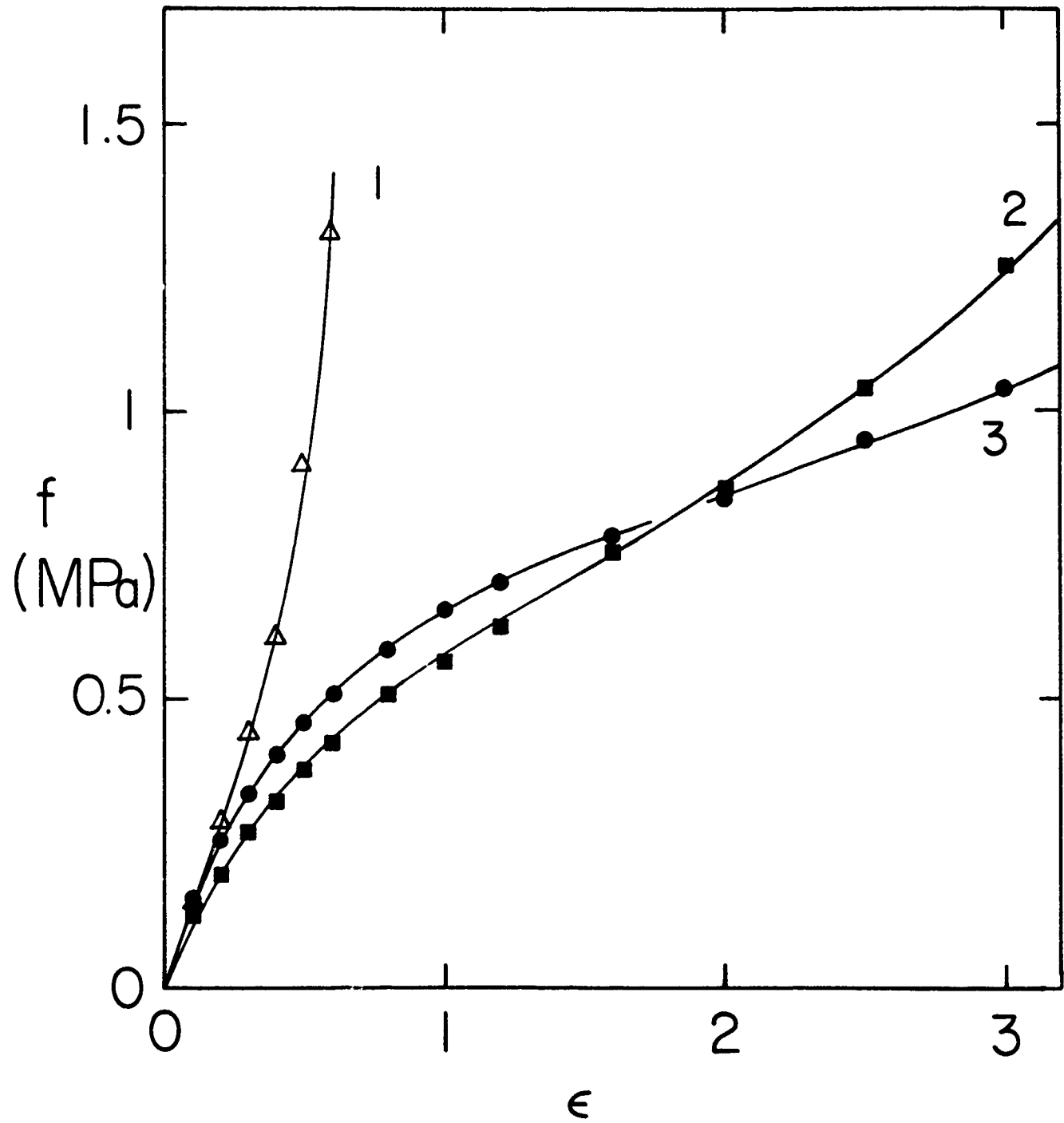


Figure 3.

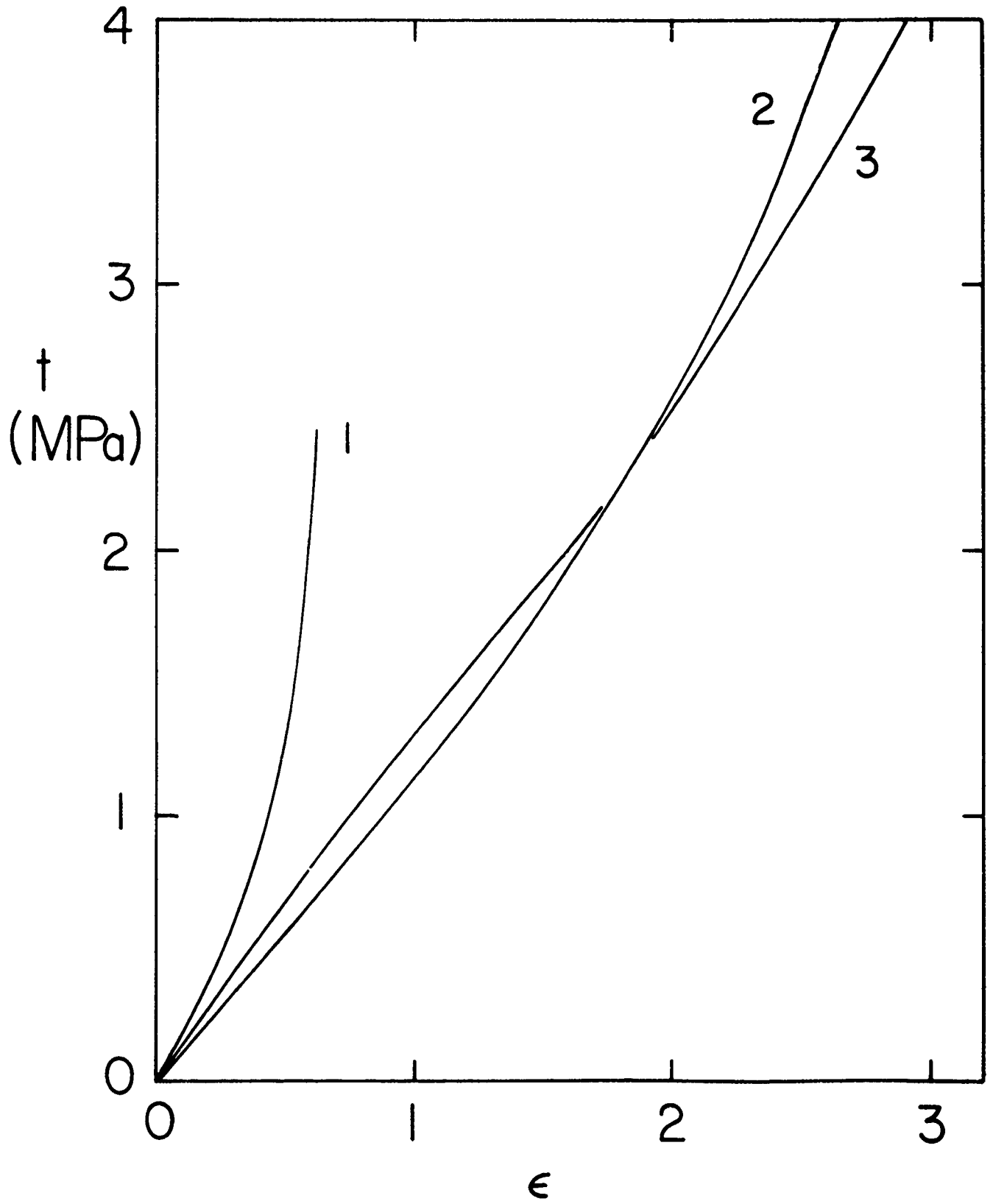
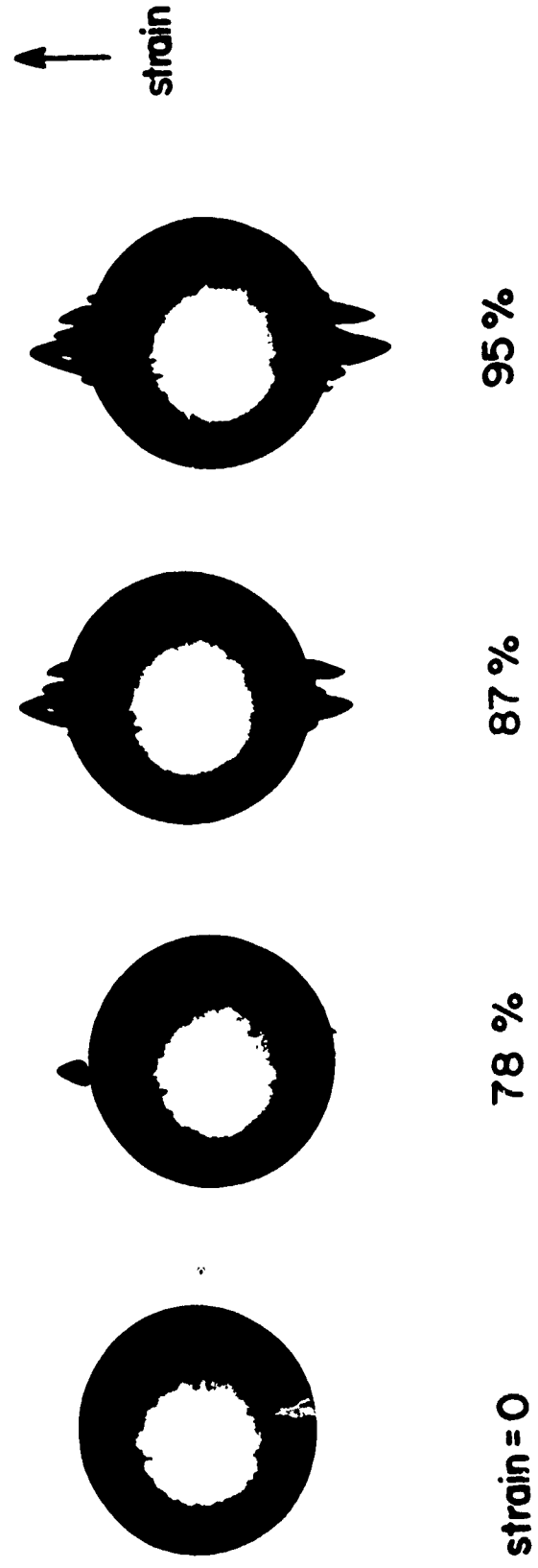


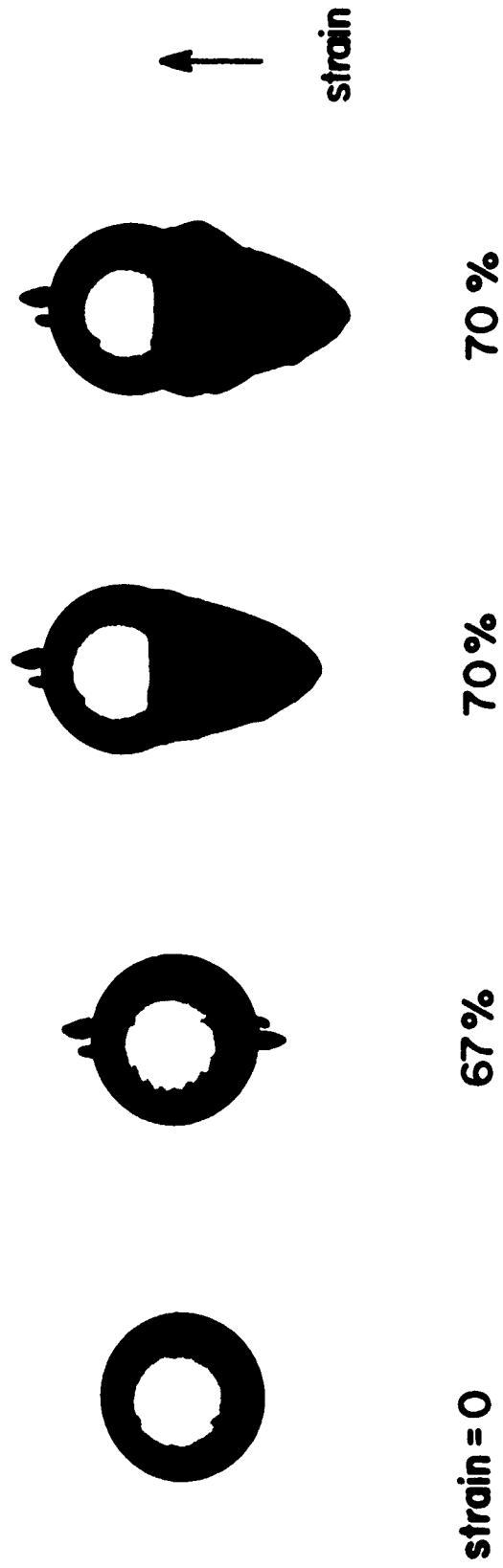
Figure 4.

Sequence of Cavitation Phenomenon under Uni-axial Loading



a glass bead ($d=1220\mu\text{m}$) treated with a primer in silicone elastomer ($E=0.88\text{ MPa}$)

Sequence of Failure Phenomena under Uniaxial Loading



a glass bead ($d=610\mu\text{m}$), untreated, in silicone elastomer ($E=2.25\text{ MPa}$)

Sequence of Debonding Phenomenon under Uni-axial Loading

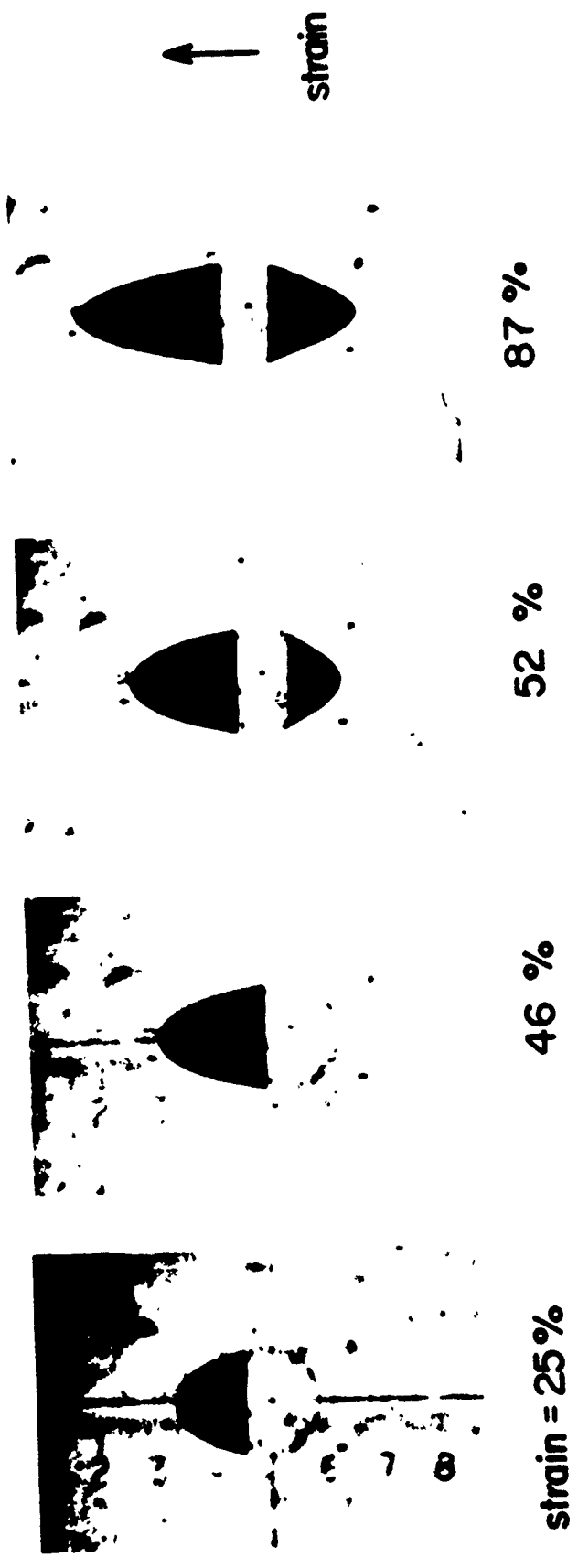


Figure 7.

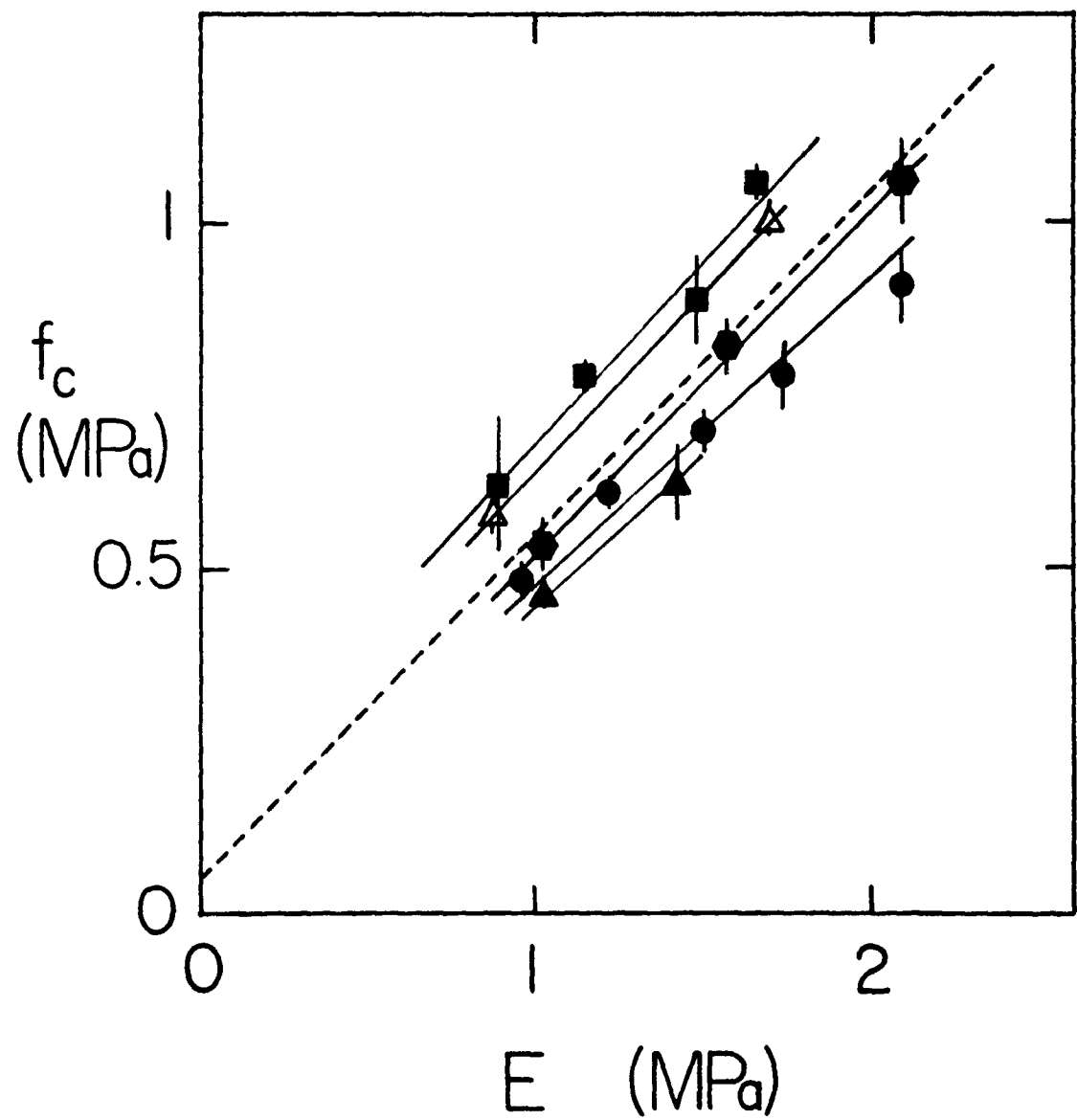


Figure 8.

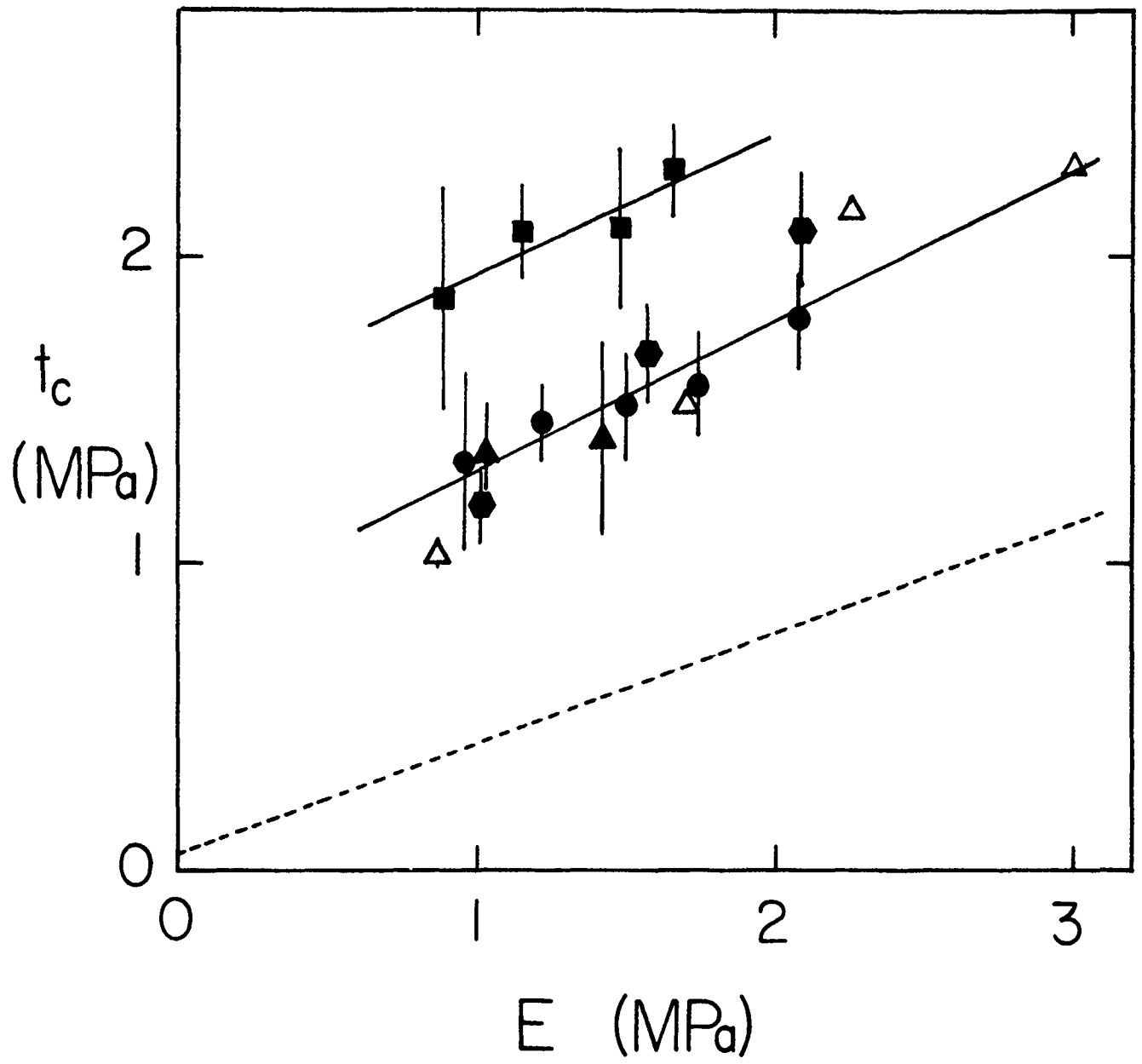


Figure 9.

Applied Stress t_c For Void Formation vs. Tensile Modulus E

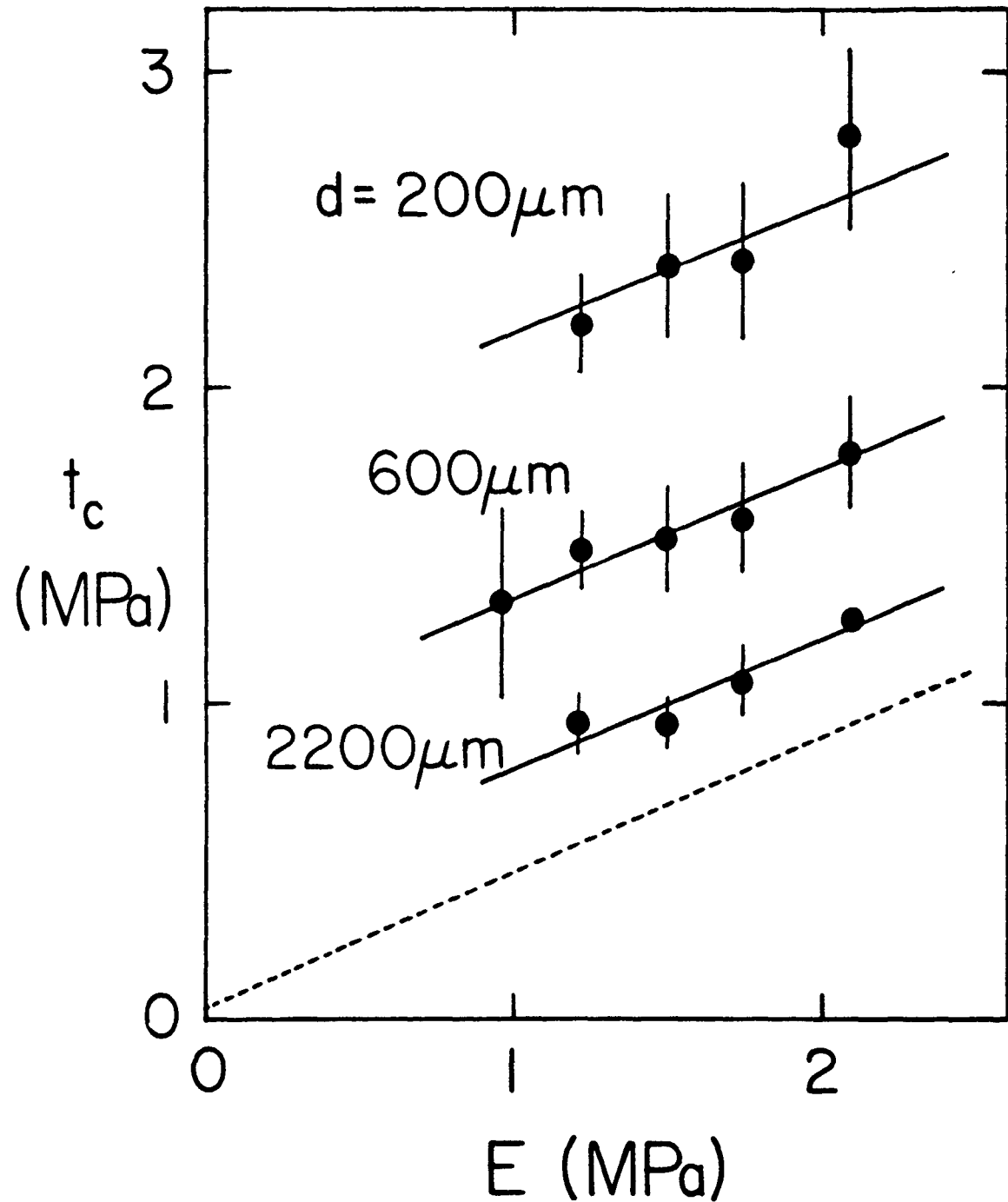


Figure 10.

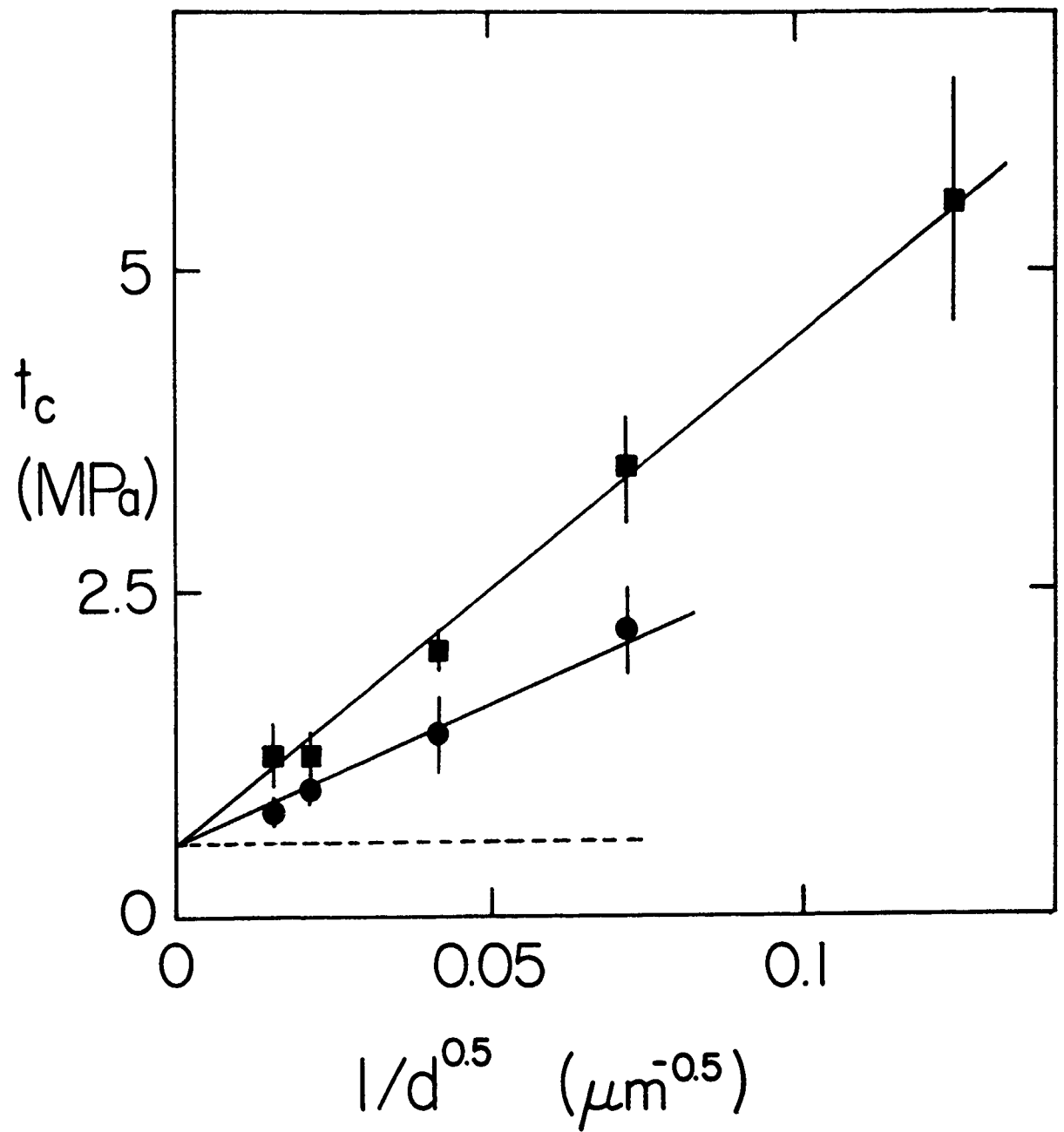


Figure 11.

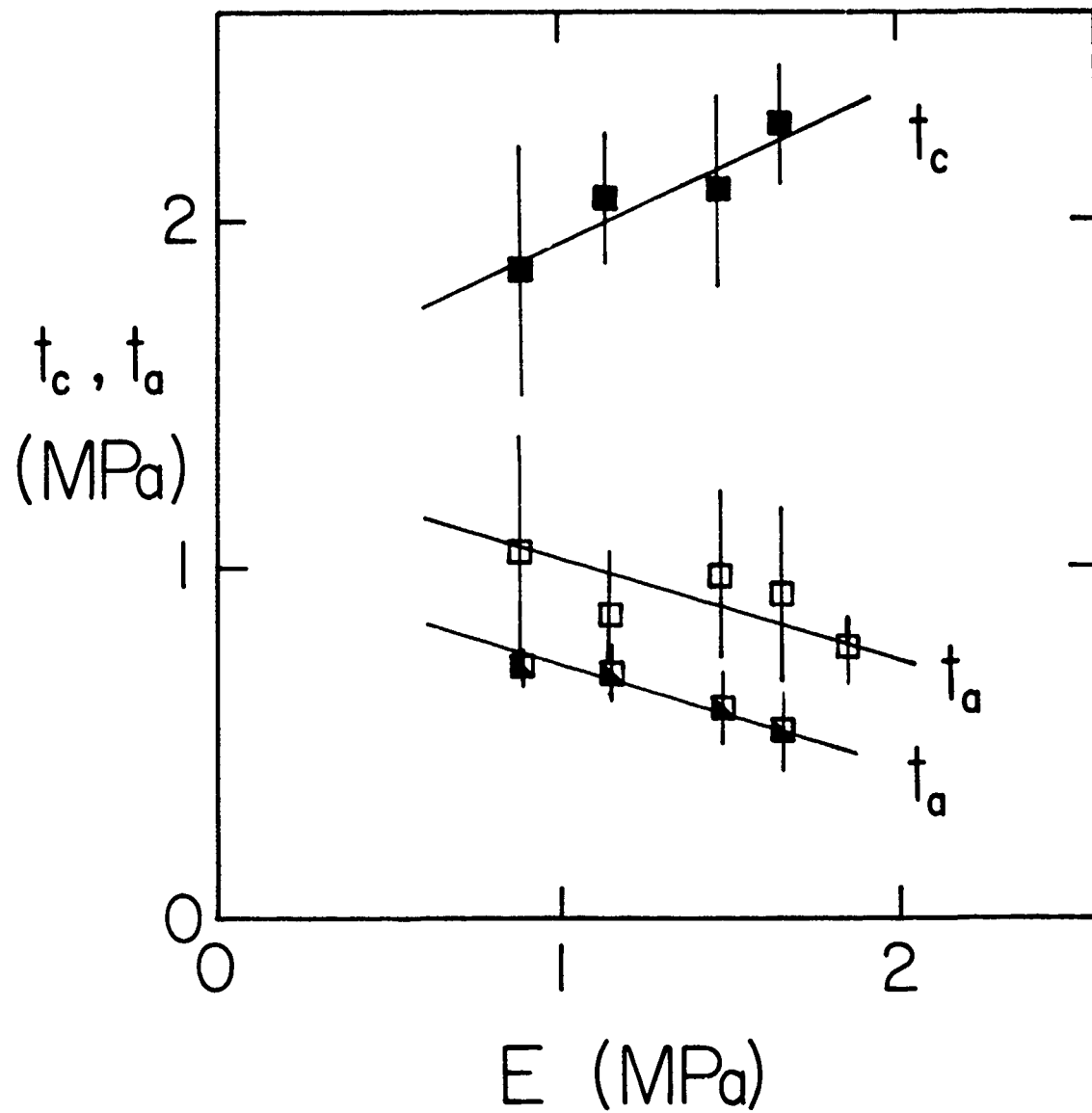


Figure 12.

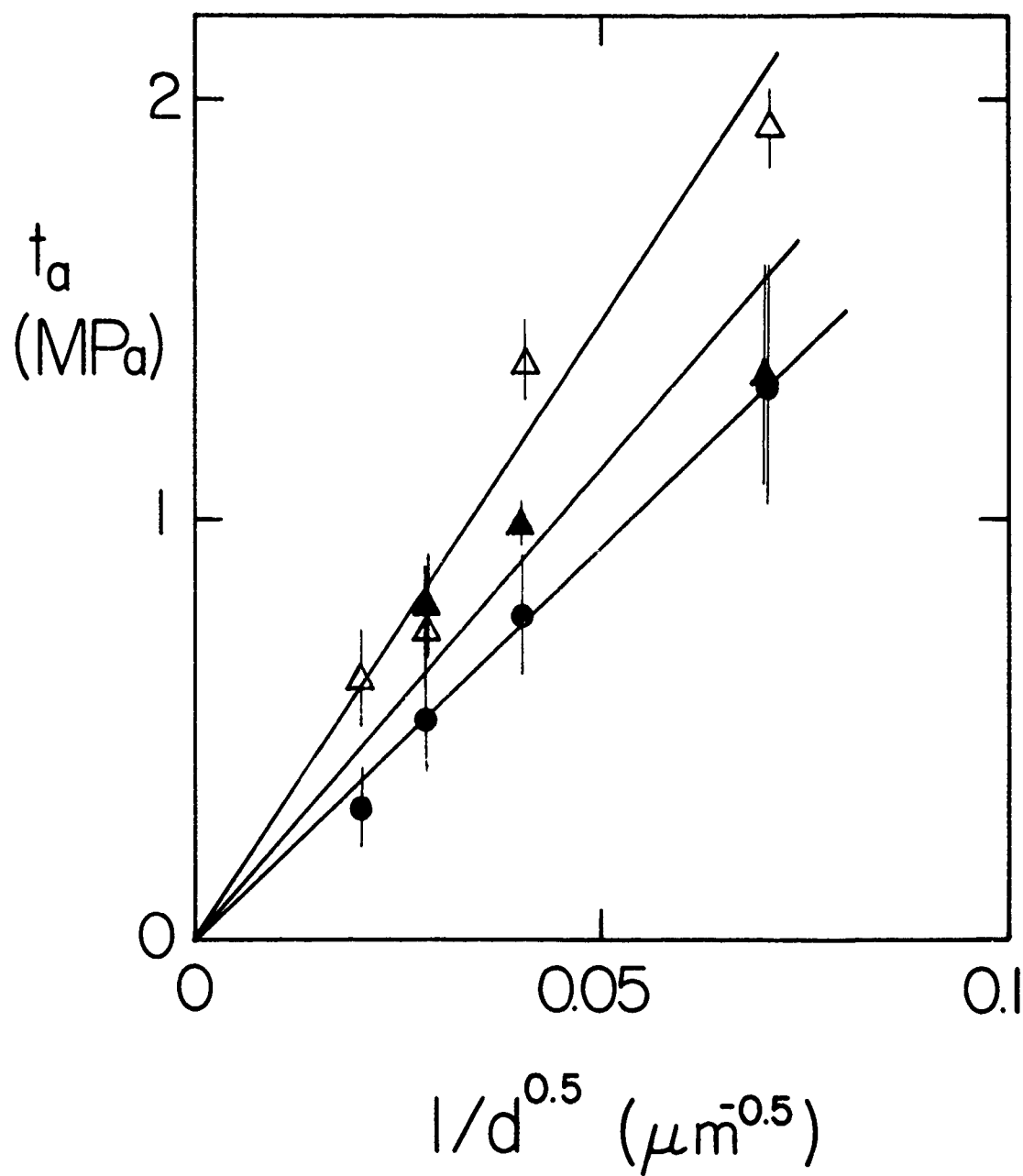


Figure 13.

Failure Phenomena in the Presence of Two Inclusions

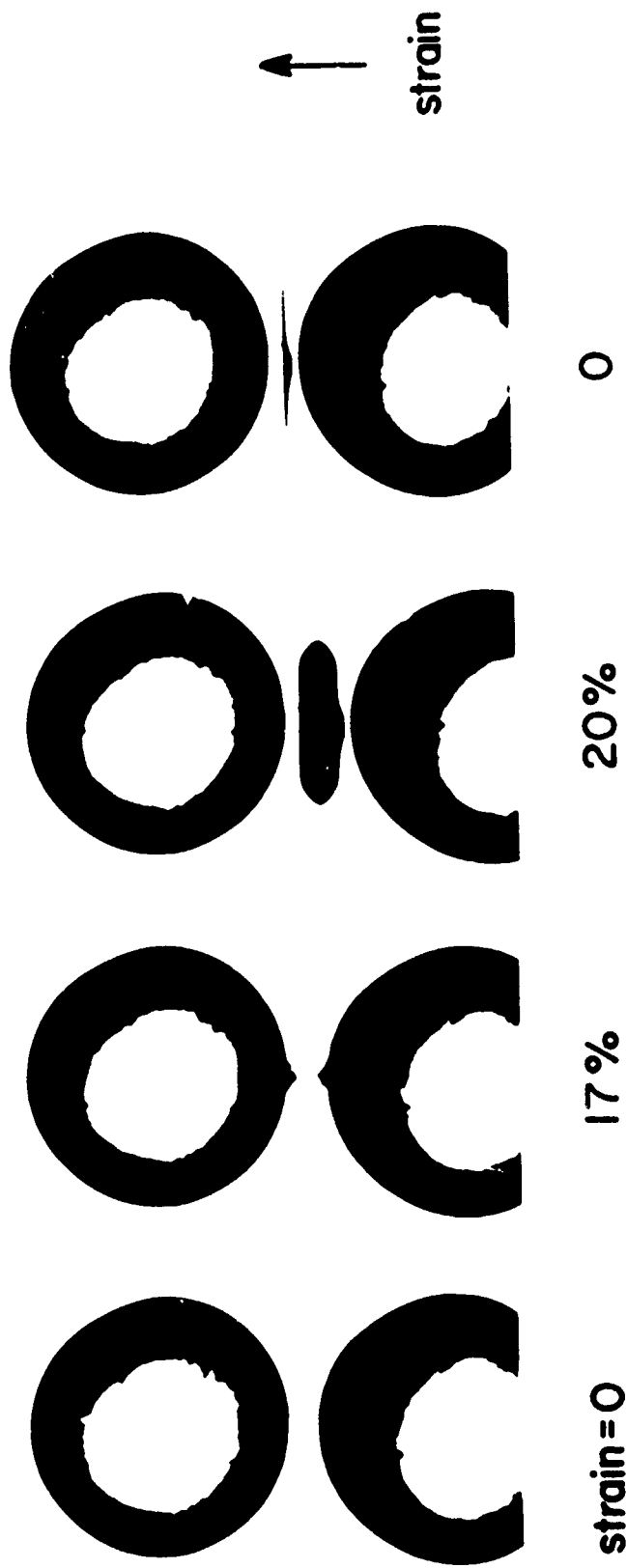


Figure 14.

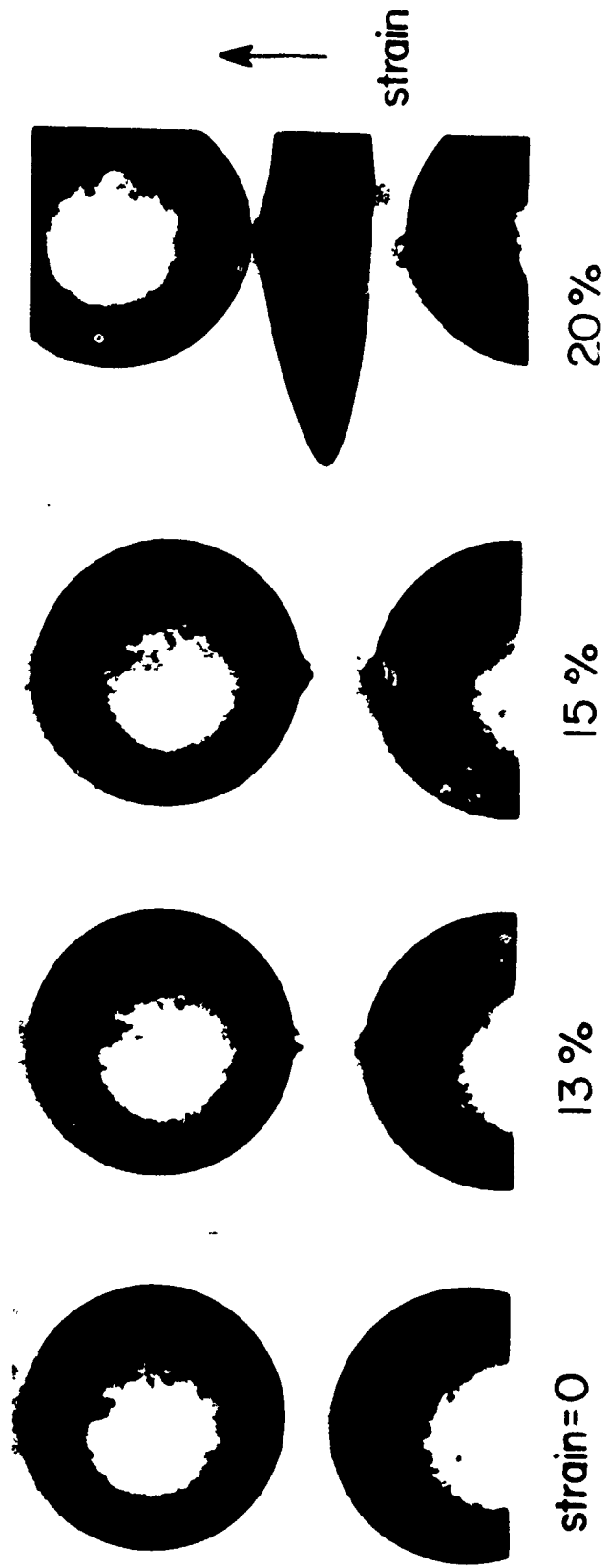


Figure 15.